Article

Cell Reports

Melanin Pathway Genes Regulate Color and Morphology of Butterfly Wing Scales

Graphical Abstract

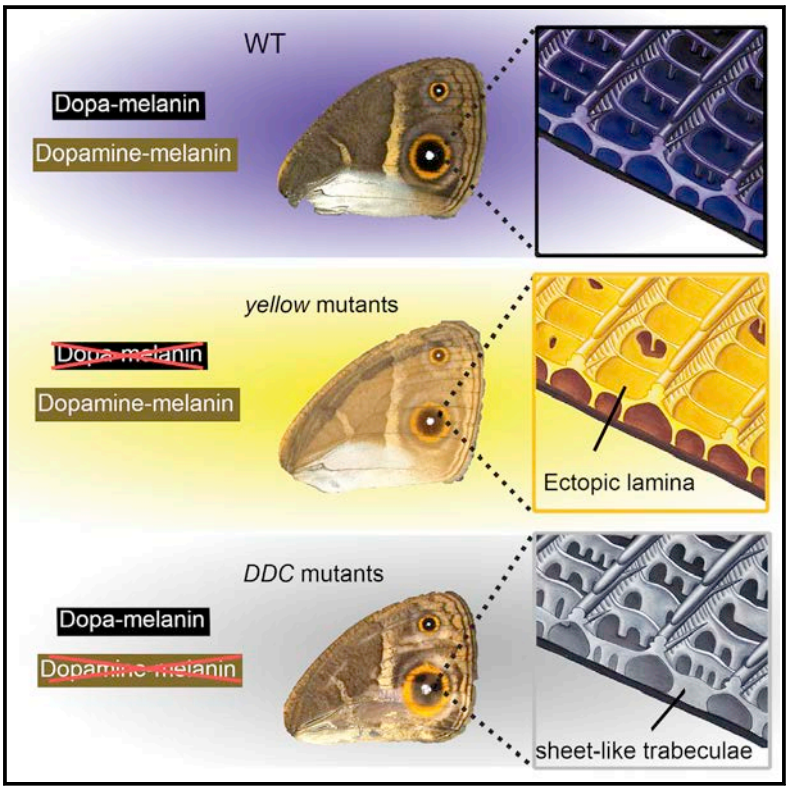

Authors

Yuji Matsuoka, Antónia Monteiro

Correspondence

dbsyuji@nus.edu.sg (Y.M.),
antonia.monteiro@nus.edu.sg (A.M.)

In Brief

Matsuoka and Monteiro discover that deletions of the *yellow* and *DDC* melanin genes alter both the color and the morphology of *Bicyclus anynana* wing scales. This study identifies genes that regulate the intricate morphology of wing scales.

Highlights

- Melanin pathway products regulate both the color and morphology of butterfly wing scales
- The link between color and morphology underscores a potential bias and/or constraint
- Different melanin genes and/or products produce each color on the wings of *Bicyclus anynana*
- Female wing scales are larger than male wing scales

Matsuoka & Monteiro, 2018, Cell Reports *24*, 56–65
July 3, 2018
https://doi.org/10.1016/j.celrep.2018.05.092

CellPress

OPEN ACCESS
CellPress

Cell Reports
Article

Melanin Pathway Genes Regulate Color and Morphology of Butterfly Wing Scales

Yuji Matsuoka[1,*] and Antónia Monteiro[1,2,3,*]
[1]Department of Biological Sciences, National University of Singapore, 14 Sciences Drive 4, Singapore 117543, Singapore
[2]Science Division, Yale-NUS College, 10 College Avenue West, Singapore 138609, Singapore
[3]Lead Contact
*Correspondence: dbsyuji@nus.edu.sg (Y.M.), antonia.monteiro@nus.edu.sg (A.M.)
https://doi.org/10.1016/j.celrep.2018.05.092

SUMMARY

The cuticular skeleton of a butterfly wing scale cell is an exquisitely finely sculpted material that can contain pigments, produce structural colors, or both. While cuticle rigidity and pigmentation depend on the products of the melanin pathway, little is known about whether genes in this pathway also play a role in the development of specific scale morphologies. Here, we use CRISPR/Cas9 to show that knockout mutations in five genes that function in the melanin pathway affect both the fine structure and the coloration of the wing scales. Most dramatically, mutations in the *yellow* gene lead to extra horizontal laminae on the surface of scales, whereas mutations in *DDC* gene lead to taller and sheet-like vertical laminae throughout each scale. We identify genes affecting the development of color and scale morphology, the regulation and pleiotropic effects of which may be important in creating and limiting the diversity of the structural and pigmentary colors observed in butterflies.

INTRODUCTION

The exoskeleton of insects provides important structural support and is used as a canvas for the deposition of pigments or for the sculpting of structural colors used in camouflage and mate signaling. The skeleton is made up of cuticle, an extracellular matrix comprising chitin fibers, cuticular proteins, lipids, and pigments (Moussian, 2010). One of the most common pigments found in insect cuticle is melanin, and some melanin pathway products also take part in cuticle hardening or sclerotization, causing cuticular melanization in insects to be tightly linked with cuticular sclerotization. For example, the cross-linking of melanin pathway molecules with nucleophilic amino acid residues and cuticular proteins confers cuticle stiffness (Xu et al., 1997; Kerwin et al., 1999; Andersen, 2005; Suderman et al., 2006; Noh et al., 2016). The interaction among all of these cuticle components is therefore important in the assembly of the insect exoskeleton and in its coloration (Xiong et al., 2017).

Given the interdependency of coloring and hardening cuticle we sought to explore whether mutations in the enzymes that control the flux of chemical precursors across pigment biosynthetic pathways affect both the spatial patterns of cuticle deposition and its coloration.

We chose to examine the effects of pigment enzyme mutations on both the color and intricate morphology of butterfly wing scales because scales of different color within a wing often display different cuticular micromorphologies (Ghiradella et al., 1972; Vukusic et al., 2000; Janssen et al., 2001; Stavenga et al., 2004; Siddique et al., 2015). This suggests that the two processes may be linked genetically. Furthermore, scale pigmentation and morphological patterning coincide during pupal wing development. For instance, melanin pigments are deposited at late pupal development stages, with a subtle time lag between the deposition of yellow, brown, and black melanin pigments (Koch et al., 1998; Wittkopp and Beldade, 2009), and this process correlates with the development of the fine morphological features of scales such as the longitudinal ridges and crossribs (Waku and Kitagawa, 1986; Ghiradella, 1989) (Figure 1). In addition, most melanin pigmentation enzymes are expressed at these same late stages (Nishikawa et al., 2013; Connahs et al., 2016; Zhang et al., 2017a), indicating that they may play a dual role in scale construction and pigmentation. We hypothesized, therefore, that molecules that determine color in butterfly wings also may regulate scale morphology.

We focused on enzymes from two main pigmentation pathways, the melanin pathway and the ommochrome synthesis pathway. The melanin biosynthetic pathway comprises a well-studied branched series of chemical reactions that can produce five different final molecules: two types of eumelanin (dopa-melanin and dopamine-melanin), pheomelanine, *N*-β-alanyldopamine (NBAD), and *N*-acetyldopamine (NADA) (Galván et al., 2015; Arakane et al., 2009; Figure 2A). Eumelanins are made from dihydroxyphenylalanine (DOPA) or from dopamine through additional reactions catalyzed by the *laccase2* and *yellow* family gene products to produce black (dopa-melanine) and brown (dopamine-melanin) pigments (Andersen, 2005; Figure 2A). Recently, pheomelanine (a reddish-yellow pigment) was identified as an additional final product of the melanin pathway in insects (Speiser et al., 2014; Galván et al., 2015; Jorge García et al., 2016; Polidori et al., 2017; Figure 2A). NBAD and NADA are sclerotizing precursor molecules that have a yellow color and are colorless, respectively. These molecules are made from dopamine through a reaction catalyzed by the *ebony* gene product and the *aaNAT* gene product, respectively (Figure 2A). The ommochrome pathway typically produces yellow, orange, and red pigments (Reed et al., 2008; Ferguson and Jiggins, 2009). The *vermilion* gene product, tryptophan oxidase, is

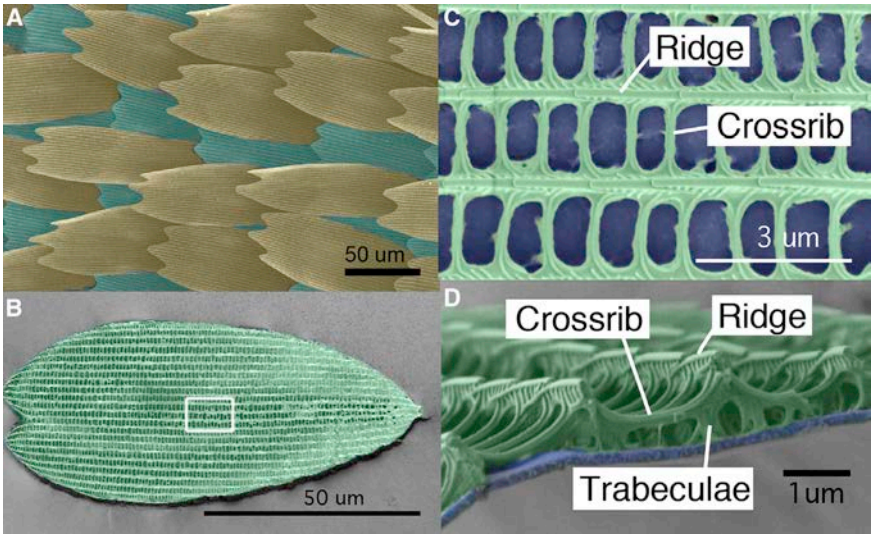

Figure 1. Wing Scale Arrangement and Scale Structure of *B. anynana*

(A) Arrangement of butterfly wing scales with cover (tan) and ground (green) scales alternating along vertical rows.

(B) Individual ground scale, where the white square indicates the region magnified in (C).

(C) Ridges run along the longitudinal axis of the scale and crossribs connect neighboring ridges, resulting in the delineation of open spaces, or windows (blue).

(D) Cross-sectional view of a similar area as in (C), showing a smooth lower lamina (blue) and a more intricately patterned upper lamina (green). The upper lamina connects to the lower lamina via the trabeculae.

Scales and features of scales are artificially colored.

the most upstream enzyme in the pathway, whereas *white* and *scarlet* code for a transporter protein that allow ommochrome pigment precursors to be incorporated into pigment granules (Mackenzie et al., 2000; Figure 2B).

We chose to examine the functions of five melanin and three ommochrome biosynthesis genes in controlling the color and morphology of the wing scales of *Bicyclus anynana*, an African butterfly (Lepidoptera; Nymphalidae; Satyrinae). The brown, beige, black, and gold colors on the wings of *B. anynana* likely result from pigments in these pathways (Figure 2). We first examined differences in scale color and morphology across the sexes. Then, we used CRISPR/Cas9 to knock out these eight genes. Recent CRISPR/Cas9 mutagenesis in *B. anynana* as well as in other butterfly species targeted a few melanin genes and a candidate ommochrome regulator, and color disruptions were reported in all of the species (Zhang et al., 2017a, 2017b). Here, in addition to the previously described color disruptions in *yellow* and *ebony* in *B. anynana* (Zhang et al., 2017a), we targeted the function of three other melanin biosynthesis pathway genes, *tyrosine hydroxylase* (*TH*), *DOPA decarboxylase* (*DDC*), and *arylalkylamine N-acetyltransferase* (*aaNAT*), and three ommochrome biosynthesis pathway genes, *vermilion, white*, and *scarlet,* with the aim of identifying the enzymes and biosynthesis products needed for generating each of the scale colors in *B. anynana*. Finally, we examined whether some of these enzymes and molecules contribute to both color and morphology of scales.

RESULTS

Morphology but Not Color Differs between Male and Female Scales

Before conducting analyses on pigment biosynthesis gene mutants, we analyzed the differences between wild-type male and female scales. The scales of *B. anynana* represent typical butterfly scales, containing a smooth lower lamina and a more intricately patterned upper lamina with longitudinal ridges that run along the proximal-distal (P-D) axis and connect to the lower lamina via short pillars called trabeculae (Ghiradella and Radigan, 1976; Wasik et al., 2014) (Figure 1). Each longitudinal ridge is connected via thinner crossribs, resulting in the delineation of open spaces, or windows (Figure 1). Butterflies also have two types of scales, cover and ground, that alternate along a row and can differ in both structure and pigmentation. We found that brown and beige scales have much larger window sizes than do eyespot-forming scales (white, black, and gold) (Figure S1F; Table S4). We then examined each of these scale types independently in each sex. We found a variety of differences between the sexes in scale size and morphology but no difference in color (Figure S1; Table S4). The trend was similar in ground scales (Figure S2; Table S5). Based on these results, we decided to focus exclusively on males for the subsequent study of the effects of mutations of melanin and ommochrome pathway genes on color and scale morphology.

Targeted Mutagenesis against Melanin and Ommochrome Biosynthesis Genes

Using CRISPR/Cas9 we disrupted the functions of five melanin biosynthesis pathway genes—*TH, DDC, yellow, ebony*, and *aaNAT*—and three ommochrome pathway genes—*vermilion, white*, and *scarlet* (injection details, numbers, etc., are summarized in Table S1). Single-guide RNA (sgRNA) activity was confirmed as seen in Figure S3. We scored phenotypes in G_0 mosaic individuals.

TH *Mutants*

TH catalyzes tyrosine into DOPA, which is the initial step of the melanin pathway (Figure 2A). Removing TH function is known to eliminate all of the melanin pathway products in a variety of arthropods, including in *B. anynana* (True et al., 1999; Liu et al., 2010, 2014; Zhang et al., 2017a; Figure 2A). Of 21 larvae, 3 showed a lack of black pigment on the head capsule, which is usually black in the first and second instars (Figure S4A). Three out of six butterflies successfully emerged from pupae. Wing scales of all colors were missing in some of the *TH* mutant clones (Figure 3A). In other clones (perhaps heterozygous clones with a single copy of *TH* mutated), scales were present but had less pigment and were curled. White scales, even in

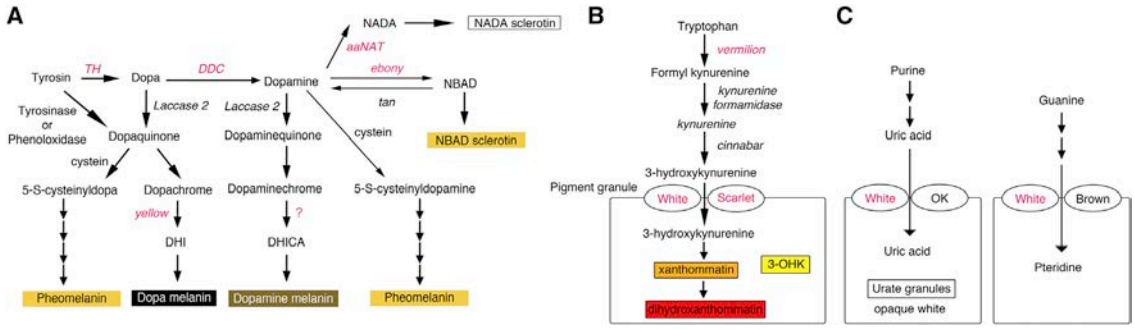

Figure 2. Proposed Melanin and Ommochrome Biosynthesis Pathways in Insects

(A) The melanin biosynthesis pathway produces up to five different molecules: pheomelanin, dopa-melanin, dopamine-melanin, NADA sclerotin, and NBAD sclerotin. NADA and NBAD sclerotin contribute to the sclerotization of cuticle when cross-linked with cuticular proteins. Dopa-melanin and dopamine-melanin are thought to be generated by the oxidative polymerization of 1-carboxyl 5,6-dihydroxyindole-2-carboxylic acid (DHI) and 5,6-dihydroxyindole (DHICA), respectively. Pheomelanin is generated by the oxidative polymerization of cysteinyldopa or cysteinyldopamine in the presence of cysteine (Ito and Wakamatsu [2008]). The scheme is modified from Galván et al. (2015) and Arakane et al. (2009).

(B) The ommochrome pathway produces up to three different pigments: 3-hydroxykynurenine (3-OHK), xanthommatin, and dihydroxanthommatin.

(C) Functional redundancy of ABC transporter proteins. The White transporter protein also can form heterodimers with OK and Brown to incorporate different precursors into the pigment granule used in the production of other pigments such as urate granules or pteridines. Highlighted in red are the enzymes investigated in this study.

putatively heterozygous clones that are contiguous with other colored regions, were affected in more extreme ways and were always absent. Together, these results indicate that *TH* is required for larval head pigmentation and for scale overall development, pigmentation, and structural rigidity. These phenotypes are similar to those observed in other butterfly species (Zhang et al., 2017a).

DDC *Mutants*

DDC catalyzes the production of dopamine from DOPA (Figure 2A). By disrupting the function of DDC, butterflies are expected to be able to produce only dopa-melanin (black pigment); however, they may still be able to produce pheomelanin if that part of the pathway is active in *B. anynana* wing scale cells. 5 out of 42 larvae lacked black pigment on their heads (Figure S4A). From two of the seven butterflies that emerged, the black eyespot scales became gray, the brown and beige scales became whitish, the gold ring region became paler while still retaining a gold color, and the white eyespot center scales were absent (Figure 3A). Furthermore, all of the scales were mostly curled. All of these phenotypes were similar to the mild *TH* mutant phenotypes. L*a*b color space quantitative analyses (Hirschler, 2010) supported the visible color changes described: *DDC* mutant scales, other than beige scales, were significantly lighter (higher L value) and less yellowish in color (lower b value) compared to wild-type (WT) scales (Figure 3C; Table S6). Our results indicate that dopamine is an important precursor for the pigments contained in most wing scales and a required molecule in the development of white scales. The persistence of black and gold pigments in the black and gold mutated scales, respectively, indicate that dopa-melanin is likely present in the black scales, and other non-dopamine-derived pigments (possibly pheomelanin or an ommochrome pigment) are present in the gold scales. These results also indicate that *DDC,* similar to *TH,* is required for scale hardening across all of the colored scales.

aaNAT *Mutants*

aaNAT catalyzes the conversion of dopamine to NADA sclerotin (colorless) (Figure 2A). WT *B. anynana* naturally change their head capsule color from black in the third instar to light brown in the fourth instar (Figure S4B). From 20 larvae showing a normal black head as third instars, 16 retained their black head capsule color until the last larval instar (Figure S4B). This phenotype is similar to the phenotype observed in *Bombyx aaNAT* RNAi larvae (Long et al., 2015). 4 out of 20 butterflies lacked white scales in multiple eyespot centers (Figure 3A), but no other scale abnormalities were detected. These results indicate that *aaNAT* is required for brown head capsule pigmentation in late larvae, the lighter color achieved presumably by shunting DOPA away from dopa-melanin production and into NADA sclerotin production. *aaNAT* also is required for the development of the white, structurally colored scales of the eyespot centers.

yellow *and* ebony *Mutants*

Color changes in both *yellow* and *ebony* mutants in *B. anynana* were previously broadly described (Zhang et al., 2017a), but here we quantified those changes using the L*a*b color space analysis. In *yellow* mutants, the darker-colored scales (black and brown) became significantly lighter relative to WT scales, whereas the lighter-colored scales (gold, beige, and white) did not change in color (Figures 3A and 3C; Table S6). This indicates that *yellow* is active only in darker-colored scales. We infer that in these scales *yellow* is acting to convert DOPA to dopa-melanin.

In *ebony* mutants the result was opposite that of *yellow* mutants; in other words, the lighter-colored scales (gold and beige) became significantly darker relative to WT scales, whereas the darker-colored scales (black and brown) did not change in color (Figure 3A). This indicates that ebony is active only in the lighter-colored scales to convert dopa-melanin to NBAD sclerotin (yellow). The removal of *ebony* makes these scales less yellow (lower b) and darker (lower L) (Figure 3C; Table S6).

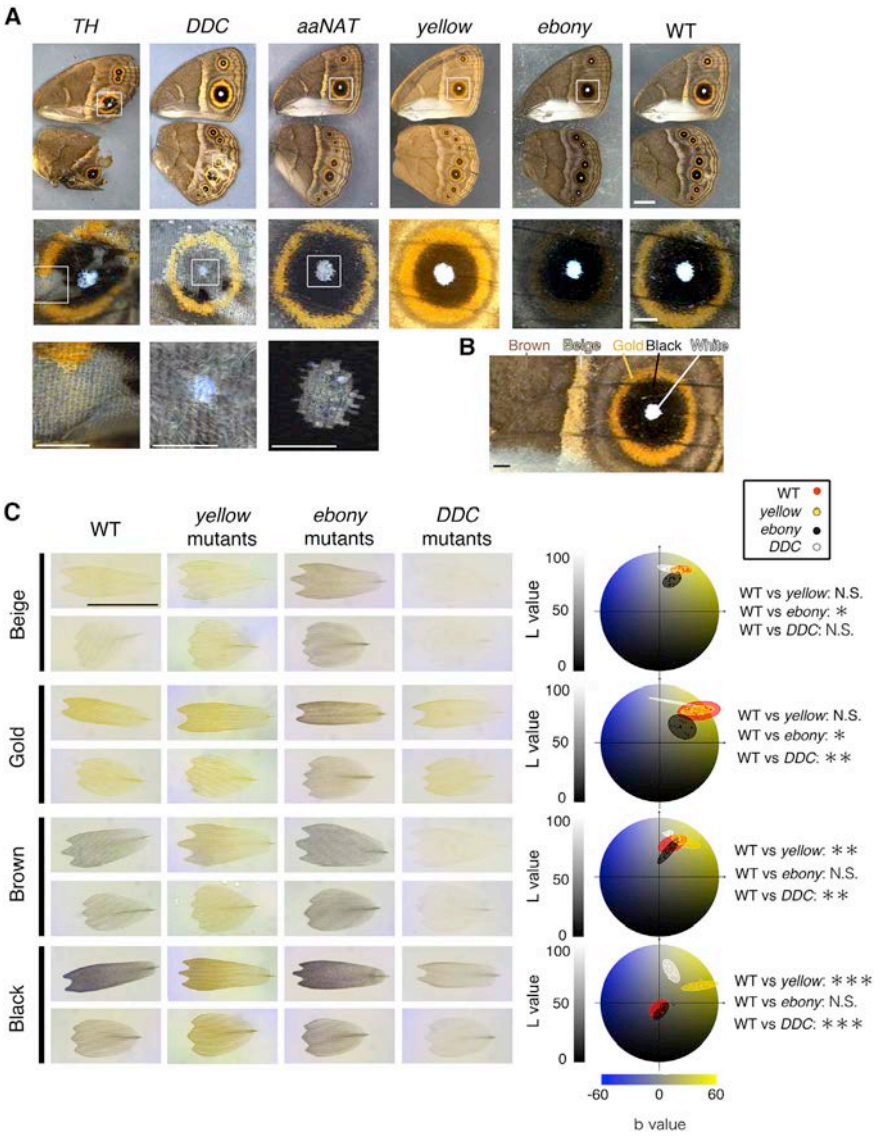

Figure 3. Melanin Biosynthesis Gene Mutants in *B. anynana*

(A) Representative pictures of each melanin gene mutant. *TH*, scales of all colors failed to develop in mutant *TH* clonal tissue. *DDC*, scale development also was disrupted but not as frequently as in *TH* mutants. White scale development was always disrupted in mutant clones, but gold, brown, and black scales became paler and curled in presumed heterozygous mutant clones. In *aaNAT* mutants, white scale development alone was disrupted. In *yellow* mutants, brown and black scales became lighter, and in *ebony* mutants, beige and gold scales became darker. Scale bar indicates 5 mm in low-magnification images (top row) and 1 mm in higher-magnification images (middle and bottom rows).

(B) Colored areas that were sampled for individual scale measurements. Scale bar indicates 1 mm.

(C) Transmission photos of individual mutant and wild-type (WT) cover and ground scales. Scale bar indicates 100 μm. Diagrams at right show the color space occupied by cover scales on the L*a*b color space. Each colored ellipse represents measurements from five scales from three different male individuals (N = 3 for statistical analyses). *$p \leq 0.05$, **$p \leq 0.01$, and ***$p \leq 0.001$. See also Figures S3 and S4 and Tables S1 and S6.

Ommochrome Biosynthesis Pathway May Not Contribute to Wing Coloration in B. anynana

To examine whether the ommochrome pathway contributes to the production of the gold color in *B. anynana*, we individually disrupted the function of three ommochrome biosynthesis pathway genes, *vermilion, white*, and *scarlet*. The vermilion gene product catalyzes the most upstream reaction of ommochrome pathway while White and Scarlet are ATP-binding cassette (ABC) transporters that form heterodimers to selectively incorporate the ommochrome precursor into the pigment granules inside cells (Mackenzie et al., 1999; Figure 2B). We confirmed the presence of indel mutations in groups of embryos, after injection of sgRNA targeting each of these genes along with Cas9 (Figure S3), but we did not observe any wing phenotypes in adults. The *white* mosaic mutants, however, showed disruption of larval body color and lack of pigmentation in the adult eyes (Figures S4B and S4C). Lack of eye pigmentation also was observed in a single adult eye of a *scarlet* mosaic mutant (Figure S4C). We did not detect any phenotypes from *vermilion* mutants in larvae or adults, even though a previous study detected *vermilion* expression in developing wing tissue in this species (Beldade et al., 2005).

Deletion of Melanin Pathway Genes Affected Scale Morphology

To examine the contribution of melanin biosynthesis pathway products to the development of scale size and the cuticular microstructures of wing scales, we took scanning electron microscopy (SEM) images of individual scales of different colors from male mutants and compared these to WT scales. In *yellow* mutants, the windows of the black and brown scales were covered broadly by a supernumerary lamina (Figure 4A), which only rarely occurs in WT scales, with the exception of white scales, which naturally display parts of such lamina. White, gold, and beige scales showed no marked differences in these mutants. The crossribs flanking these closed windows in mutant scales were thinner and the crossrib spacing was significantly denser in black and brown scales (Figure 4B; Tables S9 and S10). The overall scale size and the distance between longitudinal ridges were unchanged (Figure 4B; Tables S7 and S8).

In *DDC* mutants, the arrangement of crossribs on all of the color scales became disordered, and neighboring crossribs often were fused, resulting in larger windows (Figure 4A). Sheet-like trabeculae, taller than the feet-like trabeculae of WT

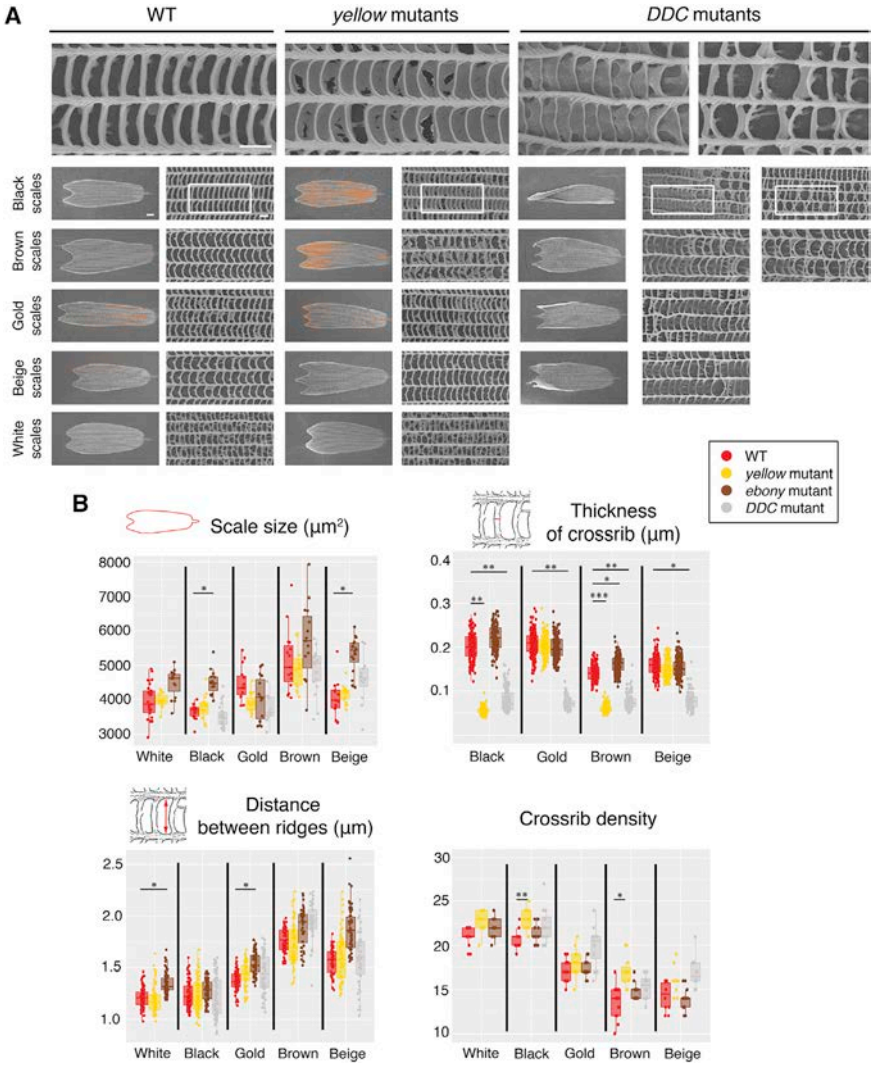

Figure 4. Scanning EM Images of Individual Scales from WT, *yellow*, and *DDC* Mutants and Detailed Morphological Measurements from These and *ebony* Mutants

(A) Representative images of individual scales from WT, *yellow* mutants, and *DDC* mutants. In *yellow* mutants, there is a thin lamina that covers the windows of darker-colored scales (black and brown) (the ectopic lamina was colored in orange in the scanning EM images). The morphology of the lighter-colored scales (gold, beige, and white) is unchanged. In *DDC* mutants, crossribs are more disorganized and sometimes fuse with neighboring crossribs. In addition, trabeculae become sheet-like underneath the crossribs. Scale bars indicate 10 μm in low-magnification images of whole scales and 1 μm in high-magnification images (top row).

(B) Several measurements of individual scale features. We plotted all of the measurements taken from five scales of the same type from three different individuals, but statistics used N = 3, where the five measurements within an individual were averaged. Error bars represent 95% confidence intervals of means. *p ≤ 0.05, **p ≤ 0.01, and ***p ≤ 0.001.

See also Figure S5 and Tables S7, S8, S9, and S10.

scales, appeared beneath the crossribs (Figure 4A). The width of each crossrib also became thinner (Figure 4B; Table S9); however, the scale size and the distance between longitudinal ridges were unchanged (Tables S7 and S8). These phenotypes were stronger in darker-colored scales (black) and weaker in lighter-colored scales (gold and beige).

In *ebony* mutants, we did not detect dramatic changes in morphology, but the scale size was slightly larger in black and beige mutant scales, the thickness of the crossribs was slightly higher in brown mutant scales, and the distance between longitudinal ridges was slightly larger in white and gold mutant scales relative to WT scales (Figure 4B; Tables S7, S8, and S9). Most of these morphological changes had a small effect size, took place in scales where there was no significant effect on color, did not transform the morphology of one colored scale into that of another colored scale, and may be simply due to slight differences in genetic background between the six animals measured.

In summary, the color and the morphology of the darker scales in *yellow* mutants and the color and morphology of all of the colored scales in *DDC* mutants were changed dramatically relative to WT scales. We also detected smaller changes in scale morphology in the *ebony* mutants, but these were small compared to the observed changes in color in the same mutants.

DISCUSSION

In this study, we generated mosaic mutants for five of the known melanin biosynthesis pathway genes and three of the ommochrome pathway genes using CRISPR/Cas9. This allowed us to identify which pigment pathway and which genes are needed for producing each of the colored scales on the wings of *B. anynana* and how these genes affect scale color and morphology.

The Role of Melanin Biosynthesis Pathway Genes in the Development of Pigmentary Colors

The melanin pathway mutants displayed both expected color alterations (i.e., those observed in similar experiments in other insects and butterflies) (True et al., 1999; Wittkopp et al., 2002; Arakane et al., 2009; Liu et al., 2010, 2014, 2016; Li et al., 2015; Perry et al., 2016; Zhang and Reed, 2016; Beldade and Peralta, 2017; Zhang et al., 2017a) and previously undescribed color changes. A surprising discovery was that *aaNAT* is necessary for generating the complete skeleton of white eyespot center scales in *B. anynana*, which produce a white structural color (Monteiro et al., 2015; Figure 3A). In *Bombyx*, *Oncopeltus*, and *Tribolium*, loss or downregulation of *aaNAT* caused increased cuticle melanization (Dai et al., 2010; Zhan et al., 2010; Liu

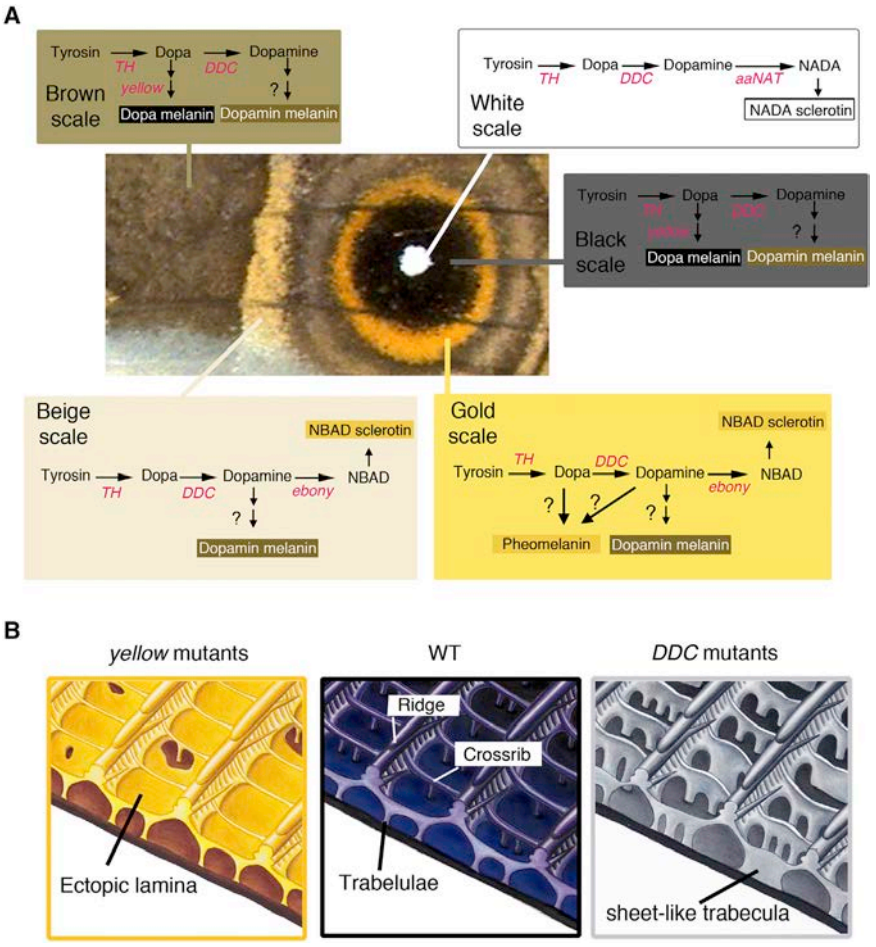

Figure 5. Cell-Specific Expression and Function of Melanin Biosynthesis Pathway Genes in Wing Scales of *B. anynana* Control Scale Color and Morphology

(A) Summary of the scale cell-specific expression of each of the examined melanin pathway genes, inferred from the loss of function mutants, on the wings of *B. anynana,* and how their combinatorial expression contributes to the production of different pigments in each scale cell.

(B) Schematic diagram of the morphology of a black scale from WT, *yellow*, and *DDC* mutants. In *yellow* mutants, black scales become yellow-brown, the normally open windows become covered by an ectopic cuticular lamina, and the adjacent crossribs become thinner, implicating the gene *yellow* in the creation of both dark pigmentation and in opening windows. In *DDC* mutants, the black scales become grayish, the trabeculae became sheet-like and taller, and the adjacent crossribs become thinner, implicating the gene *DDC* in the creation of dark pigmentation and short and pillar-like trabeculae. (Hand illustrations by Katerina Evangelou.)

et al., 2016; Noh et al., 2016). We speculate that in those systems, *aaNAT* is co-expressed with *yellow* in the same cells, leading to the redirection of the common dopamine precursor used by both enzymes to the exclusive use by *yellow*, leading to the production of more dopamine-melanin and a darker color.

The color of the gold scales in *B. anynana* was affected by mutations in *ebony* (Figure 3A), suggesting that NBAD sclerotin contributes to this color. We observed that in *DDC* mutants, gold color persisted in the affected regions. These results suggest that additional pigments also may be present in this area. We speculate that pheomelanin molecules may be contributing to this color in *B. anynana*. Despite the belief that invertebrates do not produce pheomelanin, this product was detected in mollusks, grasshoppers, butterflies, bumblebees, and wasps (Speiser et al., 2014; Galván et al., 2015; Jorge García et al., 2016; Polidori et al., 2017) and may be present in the gold wing scales of *B. anynana*.

We targeted two transporter protein genes, *white* and *scarlet,* as well as the enzyme *vermilion*. None of those ommochrome pathway gene mutations affected coloration on the wings of *B. anynana*, whereas mutations in *white* led to changes in eye and larval coloration, probably via disruptions to two other pigment pathways (Figures 2C, S4B, and S4C). ABC transporters, including White, are diverse (Merzendorfer, 2014), and different heterodimers selectively incorporate different pigment precursors into the pigment granules (Figures 2B and 2C). For instance, in *Drosophila,* the White protein forms a heterodimer with the Brown protein and incorporates a pteridine precursor into the pigment granule (Mackenzie et al., 1999; Figure 2C). The product of a *brown* gene paralog, the OK protein in *Bombyx* and *Helicoverpa* moths, forms a heterodimer with White to transport uric acid into the pigment granules of the larval epidermis to make whitish urate granules (Wang et al., 2013; Khan et al., 2017; Figure 2C). The loss of epidermal color in *white* mutants in *B. anynana* is likely due to the failure of uric acid uptake into epidermal cells as observed in *Bombyx ok* mutants (Wang et al., 2013). The eye phenotype in adult *white B. anynana* mutants can be due to a disruption in either an ommochrome precursor uptake (Mackenzie et al., 1999; Quan et al., 2002; Tatematsu et al., 2011), a pteridine precursor uptake (Dreesen et al., 1988; Grubbs et al., 2015), or a uric acid uptake (Khan et al., 2017). These results suggest that either the ommochrome pathway may not be playing a role in the development of wing pigmentation in *B. anynana* or that cells expressing these genes, especially cells of the gold ring in the eyespots, were not hit with mutations in these genes.

Color on the wings of *B. anynana* appears to derive primarily from melanin pathway products, whereas the different color patterns likely result from the different spatial expressions and perhaps also the levels of expression of the different melanin pathway genes in each scale. By examining the affected colored regions in each mutant, we inferred the spatial expression for each of these enzymes (Figure 5A) and proposed how these enzymes may be regulated by previously mapped transcription

factors. In particular, *DDC* being expressed overall on the wing and *yellow* being expressed in darker-colored scales correlates nicely with functional and quantitative *Distal-less* gene expression (Brakefield et al., 1996; Monteiro et al., 2013; Connahs et al., 2017), suggesting that *DDC* and *yellow* expression may be regulated by *Distal-less*. Any one of the 186 genes recently found to be differentially expressed in the central cells of an eyespot during the early pupal stage (Özsu and Monteiro, 2017) or at other time points (Monteiro et al., 2006; Özsu et al., 2017) could be upregulating *aaNAT* expression specifically in these cells. Expression of *ebony* in the gold ring could be upregulated by *engrailed* (Brunetti et al., 2001), but it is still unclear what could be regulating this gene in the beige transversal band. Finally, *TH* (and *DDC*) may not be spatially regulated by any of the above pattern-associated transcription factors.

Subcellular Localization and Functions of Melanin Pathway Products during Wing Scale Development

Butterfly wing scale development has been visualized largely via transmission EM (TEM) images of fixed developing scale cells (Ghiradella et al., 1972; Greenstein 1972a, 1972b; Ghiradella, 1989), but more recently fluorescent microscopy also was used (Dinwiddie et al., 2014). In TEM images of early scale development of *Ephestia kuehniella* moths, microfibril bundles, aligned with regular spacing, were observed on the surface of scale cells as the scale started to flatten (Overton, 1966; Ghiradella, 1974). Greenstein (1972b) proposed that the scale ridges of the giant silkmoth, *Hyalophora cecropia,* were likely to develop in between these microfibril bundles by buckling of the expanding extracellular cuticle. Dinwiddie et al. (2014) showed that cuticle deposition along the future longitudinal ridges happened in between flanking longitudinal actin bundles inside the developing scale, and disruption of actin filament formation led to disorganized scales. Together, these studies indicate that scale ridge development likely depends on the interaction of actin filaments and cuticle.

Our study shows that melanin pathway products also play a role during butterfly wing scale development. The development of *B. anynana* wing scales appears to require both TH and DDC, two early components of the melanin pathway that also severely affected scale sclerotization. Without *TH*, scale cells were unable to produce a cuticular skeleton (Figure 3A). Without adequate levels of either TH or DDC, scales developed a curly appearance and had overall lower levels of pigmentation. These results indicate that the expression of both genes is important in the development of the cuticular skeleton as well as in the development of melanin pigments.

The *yellow* and *DDC* mutants described here show how disruptions to the melanin synthesis pathway affect both scale color and specific details of the scale morphology (Figures 3 and 4). We infer that loss of dopa-melanin and dopamine-melanin cause the *yellow* and *DDC* color and scale structural changes, respectively. We speculate that cuticle is first distributed at the periphery of the developing scale, including in the window regions, and the presence of dopa-melanin helps cuticle polymerize around the crossribs to create windows devoid of cuticle. Similarly, cuticle would be present initially in vertical walls below the crossribs, and the presence of dopamine-melanin in these areas would help polymerize cuticle more tightly under and around each crossrib to create short and thick pillars under the ridges, the trabeculae, and thicker crossribs. At later stages, the cytoplasm of the scale cells disappears, leaving behind the cuticular skeleton (Ghiradella, 1989). Cells that do not express *DDC* leave behind tall, sheet-like trabeculae, and cells that do not express *yellow* leave behind unaggregated cuticle as a thin lamina covering the windows (Figure 5B). We propose that the polymerization and interaction of subcellular compartmentalized dopa-melanin and dopamine-melanin molecules with chitin or other cuticular proteins are important for constructing specific cuticular morphologies in the scale cell, especially involving cuticle aggregation around the trabeculae and crossribs.

Mutations in melanin pathway genes also affected scale morphology in subtler ways, such as in altering the spacing between ridges and crossribs, but these changes were not sufficient to explain why scales of different colors exhibit these different morphologies (Janssen et al., 2001; Figures S1 and S2). These results suggest that other factors besides melanin pathway products regulate these subtler quantitative differences in scale morphology between scales of different colors. Some of these factors may involve overall concentration of the cuticle inside the cell and type of cuticular proteins expressed in each scale. Ohkawa et al. (2004) demonstrated that electrospun fibers formed by lower concentrations of chitosan, a derivate of chitin, were thinner than those formed at higher concentrations. It is possible, then, that eyespot-forming scales showing a higher density of crossribs may have higher concentrations of cuticle-building materials than beige or brown scales. Finally, the amount and/or the spatial distribution of the large number of cuticle proteins found in lepidopterans (Liang et al., 2010), which have been implicated in the joint regulation of larval body cuticle thickness and its coloration (Xiong et al., 2017), also may contribute to particular scale morphologies.

By disrupting melanin and ommochrome pathway genes, we demonstrated in this study that most of the color observed on the wings of *B. anynana* comprises melanin biosynthesis pathway products. We also showed how each of the colors is the result of the expression of a specific subset of melanin pathway enzymes in each scale cell that channel the flux of precursors in the pathway into specific end pigments (Figure 5A). This work contributes to our understanding of the genetic mechanisms that establish complex color patterns in butterfly wings. We also showed that melanin biosynthesis pathway products are acting both as pigments and as scaffolds to build the fine cuticular structures of a wing scale (Figure 5B) and may therefore be important in creating as well as limiting the diversity of the structural and pigmentary colors observed in butterflies. These molecules, together with actin (Dinwiddie et al., 2014), affect the microstructures on a wing scale. The genes examined here should perhaps also be investigated in other butterflies, in particular those that show complex morphologies (Saranathan et al., 2010) and iridescent structural colors (Ghiradella et al., 1972; Vukusic et al., 2000) because they may contribute to the construction of complex photonic materials. Uncovering the genetic basis of such finely sculpted biophotonic materials may eventually pave the way for a live-cell bioengineering process of fabricating these materials.

EXPERIMENTAL PROCEDURES

Butterfly Husbandry

B. anynana, originally collected in Malawi, have been reared in the laboratory since 1988. Larvae were fed young corn plants and adults were fed mashed bananas. *B. anynana* were reared at 27°C and 60% humidity in a 12:12-hr light:dark cycle.

sgRNA Design and Production

Sequence choice for sgRNAs and sgRNA and Cas9 mRNA production was performed as previously described by Zhang et al. (2017a) and in the Supplemental Information. The sequences of sgRNAs used in this study are listed in Table S2.

Microinjection

Eggs were laid on corn leaves for 30 min. We co-injected 0.5 μg/μL final concentration of sgRNA and 0.5 μg/μL final concentration of Cas9 mRNA into embryos within 1 to 3 hr after egg laying. The eggs were sunk into PBS, and injection was performed inside the PBS. Food dye was added to the injection solution for visualization. Injected embryos were incubated at 27°C in PBS, transferred to the corn silk the next day, and further incubated at 27°C. After hatching, larvae were moved to corn leaves and reared at 27°C with a 12:12-hr light:dark cycle and 60% relative humidity.

Detection of Indel Mutations

We assessed successful disruptions of the target genes using a T7 endonuclease I assay (NEB) (in injected embryos), followed by Sanger sequencing of target regions of the DNA in adults, as previously described (Zhang et al., 2017a). Detailed procedures are described in the Supplemental Experimental Procedures. The primer sequences used in this study are listed in Table S2.

Acquisition of Colored Images

The images of butterfly wings and larvae were taken with a Leica DMS1000 microscope camera. Color images of individual scales were taken after embedding scales in clove oil. This oil matches the refractive index of the insect cuticle and allows pigmentary color to be measured precisely (Wasik et al., 2014). In particular, this oil treatment removes any contribution of structural colors that may result from light constructively interfering when crossing finely patterned materials with different refractive indexes, such as cuticle and air. We put one drop of clove oil on a glass slide. Wing scales were taken from a mutated site (from the area depicted in Figure 3B) by using a fine tungsten needle and dipped into the clove oil. Once enough scales were transferred, a cover glass was placed on top of the oil and the scales. Additional clove oil was supplied from the edge of the cover glass to fill the space, and this preparation was sealed with nail polish. Images of wing scales were taken via light transmission using an Axioskop2 mot plus (Carl Zeiss) microscope and an Axiocam ERc 5s (Carl Zeiss).

Color Measurements

Light transmission images taken using the above method were not entirely consistent for brightness, so images were edited using the Digital Color Meter (a pre-installed Macintosh application [Apple]) to make the background brightness similar across all of the images. The same relative region in a scale (in the middle) was selected with a rectangular marquee of a constant size, and the color was averaged inside the selected area using the "average" tool in Adobe Photoshop (CS3). For the quantitative assessment of color, we conducted L*a*b color space analysis, which is a way of mathematically describing color in three dimensions with three parameters. The L value (0–100) indicates how bright the color is, with higher values indicating a brighter/lighter color; the a value (−60 to 60) indicates where the color is located between red (negative values) and green (positive values) opponent colors; and the b value (−60 to 60) indicates where the color is located between blue (negative) and yellow (positive) opponent colors. The L*a*b color space is used in industry and in biological color assessment. Measurements were conducted using the Digital Color Meter. In this study, we plotted only the L and b values because the a value (red–green) was similar among all of the measured scales. Color measurements were averaged across five scales of the same color from the same individuals, and three different male and female individuals were measured for statistical purposes. ANOVAs were used to test for significant differences in mean color values between the sexes, and multivariate analyses of variance (MANOVAs) were used to test for significant differences between color of WT males and each of the male melanin mutants using IBM-SPSS Statistics version 21 software.

Scanning EM and Sample Preparation

Small pieces of wing (5 mm × 5 mm) were cut under a dissecting microscope. Fifty percent ethanol/MQ water was dropped onto the wing pieces, and the pieces were dipped into liquid nitrogen for 5 min. The wing pieces were removed from liquid nitrogen and evaporated at room temperature. The pieces of wing or individual scales were moved using a sharpened tungsten needle onto double-stick carbon tape and pressed gently onto the metal scanning EM stub. After enough desiccation (overnight), platinum conductive coating was performed for 60 s at 20 mA using an Auto Fine Coaters JFC-1600 (JEOL). Images were taken using a JSM-6701F scanning electron microscope. The method for imaging cross-sections of single scales (shown in Figure 1D) was previously described by Wasik et al. (2014).

Scale Measurements

We compared several traits between male and female scales such as area, length, width, average distance between longitudinal ribs, density of crossribs along a standard length, and width of each crossrib in both cover and ground scales of different colors. For crossrib thickness and distance between each crossrib, we took the average of 10 measurements in a different area of the scale. For distance between ridges, we took the average of three measurements in a different area of the scale. For scale area size, scale width, scale length, and scale density, we took the average of one measurement in a different area of the scale, and then the average of five individual scales of the same color from the same individual. Our sample size, for statistical purposes, was equal to 3—in other words, the measurements from three distinct individual animals of each sex. We measured each trait using ImageJ software. ANOVAs were used to test for significant differences in scale measurements between the sexes and between WT males and each of the male melanin mutants using IBM-SPSS Statistics version 21 software.

SUPPLEMENTAL INFORMATION

Supplemental Information includes Supplemental Experimental Procedures, five figures, and ten tables and can be found with this article online at https://doi.org/10.1016/j.celrep.2018.05.092.

ACKNOWLEDGMENTS

We thank Katerina Evangelou (PhD student, University of the Arts London, Central Saint Martins College, katerinaev@hotmail.com) for producing 3D hand-drawn illustrations of wing scales and also thank Monteiro Lab members for their help and discussion. The work was partially funded by the Ministry of Education, Singapore grant MOE2015-T2-2-159 and the LHK Fund from the Department of Biological Sciences, NUS (R-154-000-608-651).

AUTHOR CONTRIBUTIONS

Y.M. and A.M. designed the study. Y.M. conducted the study and analyzed the data. Y.M. and A.M. wrote the manuscript.

DECLARATION OF INTERESTS

The authors declare no competing interests.

Received: January 4, 2018
Revised: March 26, 2018
Accepted: May 29, 2018
Published: July 3, 2018

REFERENCES

Andersen, S.O. (2005). Cuticular sclerotization and tanning. In Comprehensive Molecular Insect Science, L.I. Gilbert, K. Iatrou, and S.S. Gill, eds. (Elsevier Pergamon Press), pp. 145–170.

Arakane, Y., Lomakin, J., Beeman, R.W., Muthukrishnan, S., Gehrke, S.H., Kanost, M.R., and Kramer, K.J. (2009). Molecular and functional analyses of amino acid decarboxylases involved in cuticle tanning in *Tribolium castaneum*. J. Biol. Chem. *284*, 16584–16594.

Beldade, P., and Peralta, C.M. (2017). Developmental and evolutionary mechanisms shaping butterfly eyespots. Curr. Opin. Insect Sci. *19*, 22–29.

Beldade, P., Brakefield, P.M., and Long, A.D. (2005). Generating phenotypic variation: prospects from "evo-devo" research on *Bicyclus anynana* wing patterns. Evol. Dev. *7*, 101–107.

Brakefield, P.M., Gates, J., Keys, D., Kesbeke, F., Wijngaarden, P.J., Monteiro, A., French, V., and Carroll, S.B. (1996). Development, plasticity and evolution of butterfly eyespot patterns. Nature *384*, 236–242.

Brunetti, C.R., Selegue, J.E., Monteiro, A., French, V., Brakefield, P.M., and Carroll, S.B. (2001). The generation and diversification of butterfly eyespot color patterns. Curr. Biol. *11*, 1578–1585.

Connahs, H., Rhen, T., and Simmons, R.B. (2016). Transcriptome analysis of the painted lady butterfly, *Vanessa cardui* during wing color pattern development. BMC Genomics *17*, 270.

Connahs, H., Tlili, S., van Creij, J., Loo, T.Y.J., Banerjee, T., Saunders, T.E., and Monteiro, A. (2017). Disrupting different *Distal-less* exons leads to ectopic and missing eyespots accurately modeled by reaction-diffusion mechanisms. bioRxiv. https://doi.org/10.1101/183491.

Dai, F.Y., Qiao, L., Tong, X.L., Cao, C., Chen, P., Chen, J., Lu, C., and Xiang, Z.H. (2010). Mutations of an arylalkylamine-*N*-acetyltransferase, *Bm-iAANAT*, are responsible for silkworm melanism mutant. J. Biol. Chem. *285*, 19553–19560.

Dinwiddie, A., Null, R., Pizzano, M., Chuong, L., Leigh Krup, A., Ee Tan, H., and Patel, N.H. (2014). Dynamics of F-actin prefigure the structure of butterfly wing scales. Dev. Biol. *392*, 404–418.

Dreesen, T.D., Johnson, D.H., and Henikoff, S. (1988). The brown protein of *Drosophila melanogaster* is similar to the white protein and to components of active transport complexes. Mol. Cell. Biol. *8*, 5206–5215.

Ferguson, L.C., and Jiggins, C.D. (2009). Shared and divergent expression domains on mimetic *Heliconius* wings. Evol. Dev. *11*, 498–512.

Galván, I., Jorge, A., Edelaar, P., and Wakamatsu, K. (2015). Insects synthesize pheomelanin. Pigment Cell Melanoma Res. *28*, 599–602.

Ghiradella, H. (1974). Development of ultraviolet-reflecting butterfly scales: how to make an interference filter. J. Morphol. *142*, 395–409.

Ghiradella, H. (1989). Structure and development of iridescent butterfly scales: lattices and laminae. J. Morphol. *202*, 69–88.

Ghiradella, H., and Radigan, W. (1976). Development of butterfly scales. II. Struts, lattices and surface tension. J. Morphol. *150*, 279–298.

Ghiradella, H., Aneshansley, D., Eisner, T., Silberglied, R.E., and Hinton, H.E. (1972). Ultraviolet reflection of a male butterfly: interference color caused by thin-layer elaboration of wing scales. Science *178*, 1214–1217.

Greenstein, M.E. (1972a). The ultrastructure of developing wings in the giant silkmoth, Hyalophora cecropia. I. Generalized epidermal cells. J. Morphol. *136*, 1–21.

Greenstein, M.E. (1972b). The ultrastructure of developing wings in the giant silkmoth, *Hyalophora cecropia*. II. Scale-forming and socket-forming cells. J. Morphol. *136*, 23–51.

Grubbs, N., Haas, S., Beeman, R.W., and Lorenzen, M.D. (2015). The ABCs of eye color in *Tribolium castaneum*: orthologs of the *Drosophila white, scarlet*, and *brown* genes. Genetics *199*, 749–759.

Hirschler, R. (2010). Electronic colour communication in the textile and apparel industry. file:///C:/Users/Owner/Downloads/Electronic_colour_communication_in_the_textile_and.pdf.

Ito, S., and Wakamatsu, K. (2008). Chemistry of mixed melanogenesis—pivotal roles of dopaquinone. Photochem. Photobiol. *84*, 582–592.

Janssen, J.M., Monteiro, A., and Brakefield, P.M. (2001). Correlations between scale structure and pigmentation in butterfly wings. Evol. Dev. *3*, 415–423.

Jorge García, A., Polidori, C., and Nieves-Aldrey, J.L. (2016). Pheomelanin in the secondary sexual characters of male parasitoid wasps (Hymenoptera: Pteromalidae). Arthropod Struct. Dev. *45*, 311–319.

Kerwin, J.L., Turecek, F., Xu, R., Kramer, K.J., Hopkins, T.L., Gatlin, C.L., and Yates, J.R., 3rd. (1999). Mass spectrometric analysis of catechol-histidine adducts from insect cuticle. Anal. Biochem. *268*, 229–237.

Khan, S.A., Reichelt, M., and Heckel, D.G. (2017). Functional analysis of the ABCs of eye color in *Helicoverpa armigera* with CRISPR/Cas9-induced mutations. Sci. Rep. *7*, 40025.

Koch, P.B., Keys, D.N., Rocheleau, T., Aronstein, K., Blackburn, M., Carroll, S.B., and ffrench-Constant, R.H. (1998). Regulation of dopa decarboxylase expression during colour pattern formation in wild-type and melanic tiger swallowtail butterflies. Development *125*, 2303–2313.

Li, X., Fan, D., Zhang, W., Liu, G., Zhang, L., Zhao, L., Fang, X., Chen, L., Dong, Y., Chen, Y., et al. (2015). Outbred genome sequencing and CRISPR/Cas9 gene editing in butterflies. Nat. Commun. *6*, 8212.

Liang, J., Zhang, L., Xiang, Z., and He, N. (2010). Expression profile of cuticular genes of silkworm, *Bombyx mori*. BMC Genomics *11*, 173.

Liu, C., Yamamoto, K., Cheng, T.C., Kadono-Okuda, K., Narukawa, J., Liu, S.P., Han, Y., Futahashi, R., Kidokoro, K., Noda, H., et al. (2010). Repression of tyrosine hydroxylase is responsible for the sex-linked chocolate mutation of the silkworm, *Bombyx mori*. Proc. Natl. Acad. Sci. USA *107*, 12980–12985.

Liu, J., Lemonds, T.R., and Popadić, A. (2014). The genetic control of aposematic black pigmentation in hemimetabolous insects: insights from *Oncopeltus fasciatus*. Evol. Dev. *16*, 270–277.

Liu, J., Lemonds, T.R., Marden, J.H., and Popadić, A. (2016). A pathway analysis of melanin patterning in a hemimetabolous insect. Genetics *203*, 403–413.

Long, Y., Li, J., Zhao, T., Li, G., and Zhu, Y. (2015). A new arylalkylamine *N*-acetyltransferase in silkworm (*Bombyx mori*) affects integument pigmentation. Appl. Biochem. Biotechnol. *175*, 3447–3457.

Mackenzie, S.M., Brooker, M.R., Gill, T.R., Cox, G.B., Howells, A.J., and Ewart, G.D. (1999). Mutations in the *white* gene of *Drosophila melanogaster* affecting ABC transporters that determine eye colouration. Biochim. Biophys. Acta *1419*, 173–185.

Mackenzie, S.M., Howells, A.J., Cox, G.B., and Ewart, G.D. (2000). Subcellular localisation of the white/scarlet ABC transporter to pigment granule membranes within the compound eye of *Drosophila melanogaster*. Genetica *108*, 239–252.

Merzendorfer, H. (2014). ABC transporters and their role in protecting insects from pesticides and their metabolites. Adv. Insect Physiol. *46*, 1–72.

Monteiro, A., Glaser, G., Stockslager, S., Glansdorp, N., and Ramos, D. (2006). Comparative insights into questions of lepidopteran wing pattern homology. BMC Dev. Biol. *6*, 52.

Monteiro, A., Chen, B., Ramos, D.M., Oliver, J.C., Tong, X., Guo, M., Wang, W.K., Fazzino, L., and Kamal, F. (2013). *Distal-less* regulates eyespot patterns and melanization in *Bicyclus* butterflies. J. Exp. Zool. B Mol. Dev. Evol. *320*, 321–331.

Monteiro, A., Tong, X., Bear, A., Liew, S.F., Bhardwaj, S., Wasik, B.R., Dinwiddie, A., Bastianelli, C., Cheong, W.F., Wenk, M.R., et al. (2015). Differential expression of ecdysone receptor leads to variation in phenotypic plasticity across serial homologs. PLoS Genet. *11*, e1005529.

Moussian, B. (2010). Recent advances in understanding mechanisms of insect cuticle differentiation. Insect Biochem. Mol. Biol. *40*, 363–375.

Nishikawa, H., Iga, M., Yamaguchi, J., Saito, K., Kataoka, H., Suzuki, Y., Sugano, S., and Fujiwara, H. (2013). Molecular basis of wing coloration in a Batesian mimic butterfly, *Papilio polytes*. Sci. Rep. *3*, 3184.

Noh, M.Y., Koo, B., Kramer, K.J., Muthukrishnan, S., and Arakane, Y. (2016). *Arylalkylamine N-acetyltransferase 1* gene (*TcAANAT1*) is required for cuticle

morphology and pigmentation of the adult red flour beetle, *Tribolium castaneum*. Insect Biochem. Mol. Biol. *79*, 119–129.

Ohkawa, K., Cha, D., Kim, H., Nishida, A., and Yamamoto, H. (2004). Electrospinning of chitosan. Macromol. Rapid Commun. *25*, 1600–1605.

Overton, J. (1966). Microtubules and microfibrils in morphogenesis of the scale cells of Ephestia kühniella. J. Cell Biol. *29*, 293–305.

Özsu, N., and Monteiro, A. (2017). Wound healing, calcium signaling, and other novel pathways are associated with the formation of butterfly eyespots. BMC Genomics *18*, 788.

Özsu, N., Chan, Q.Y., Chen, B., Gupta, M.D., and Monteiro, A. (2017). *Wingless* is a positive regulator of eyespot color patterns in *Bicyclus anynana* butterflies. Dev. Biol. *429*, 177–185.

Perry, M., Kinoshita, M., Saldi, G., Huo, L., Arikawa, K., and Desplan, C. (2016). Molecular logic behind the three-way stochastic choices that expand butterfly colour vision. Nature *535*, 280–284.

Polidori, C., Jorge, A., and Ornosa, C. (2017). Eumelanin and pheomelanin are predominant pigments in bumblebee (Apidae: *Bombus*) pubescence. PeerJ *5*, e3300.

Quan, G.X., Kim, I., Kòmoto, N., Sezutsu, H., Ote, M., Shimada, T., Kanda, T., Mita, K., Kobayashi, M., and Tamura, T. (2002). Characterization of the kynurenine 3-monooxygenase gene corresponding to the *white egg 1* mutant in the silkworm *Bombyx mori*. Mol. Genet. Genomics *267*, 1–9.

Reed, R.D., McMillan, W.O., and Nagy, L.M. (2008). Gene expression underlying adaptive variation in *Heliconius* wing patterns: non-modular regulation of overlapping *cinnabar* and *vermilion* prepatterns. Proc. Biol. Sci. *275*, 37–45.

Saranathan, V., Osuji, C.O., Mochrie, S.G., Noh, H., Narayanan, S., Sandy, A., Dufresne, E.R., and Prum, R.O. (2010). Structure, function, and self-assembly of single network gyroid ($I4_132$) photonic crystals in butterfly wing scales. Proc. Natl. Acad. Sci. USA *107*, 11676–11681.

Siddique, R.H., Gomard, G., and Hölscher, H. (2015). The role of random nanostructures for the omnidirectional anti-reflection properties of the glasswing butterfly. Nat. Commun. *6*, 6909.

Speiser, D.I., DeMartini, D.G., and Oakley, T.H. (2014). The shell-eyes of the chiton Acanthopleura granulata (Mollusca, Polyplacophora) use pheomelanin as a screening pigment. J. Nat. Hist. *48*, 2899–2911.

Stavenga, D.G., Stowe, S., Siebke, K., Zeil, J., and Arikawa, K. (2004). Butterfly wing colours: scale beads make white pierid wings brighter. Proc. Biol. Sci. *271*, 1577–1584.

Suderman, R.J., Dittmer, N.T., Kanost, M.R., and Kramer, K.J. (2006). Model reactions for insect cuticle sclerotization: cross-linking of recombinant cuticular proteins upon their laccase-catalyzed oxidative conjugation with catechols. Insect Biochem. Mol. Biol. *36*, 353–365.

Tatematsu, K., Yamamoto, K., Uchino, K., Narukawa, J., Iizuka, T., Banno, Y., Katsuma, S., Shimada, T., Tamura, T., Sezutsu, H., and Daimon, T. (2011). Positional cloning of silkworm *white egg 2* (*w-2*) locus shows functional conservation and diversification of ABC transporters for pigmentation in insects. Genes Cells *16*, 331–342.

True, J.R., Edwards, K.A., Yamamoto, D., and Carroll, S.B. (1999). *Drosophila* wing melanin patterns form by vein-dependent elaboration of enzymatic prepatterns. Curr. Biol. *9*, 1382–1391.

Vukusic, P., Sambles, J.R., and Lawrence, C.R. (2000). Colour mixing in wing scales of a butterfly. Nature *404*, 457.

Waku, Y., and Kitagawa, M. (1986). Developmental process of scale pigment granules in the cabbage butterfly, *Pieris rapae crucivora*. Jpn. J. Appl. Entomol. Zool. *30*, 35–42.

Wang, L., Kiuchi, T., Fujii, T., Daimon, T., Li, M., Banno, Y., Kikuta, S., Kikawada, T., Katsuma, S., and Shimada, T. (2013). Mutation of a novel ABC transporter gene is responsible for the failure to incorporate uric acid in the epidermis of ok mutants of the silkworm, *Bombyx mori*. Insect Biochem. Mol. Biol. *43*, 562–571.

Wasik, B.R., Liew, S.F., Lilien, D.A., Dinwiddie, A.J., Noh, H., Cao, H., and Monteiro, A. (2014). Artificial selection for structural color on butterfly wings and comparison with natural evolution. Proc. Natl. Acad. Sci. USA *111*, 12109–12114.

Wittkopp, P.J., and Beldade, P. (2009). Development and evolution of insect pigmentation: genetic mechanisms and the potential consequences of pleiotropy. Semin. Cell Dev. Biol. *20*, 65–71.

Wittkopp, P.J., True, J.R., and Carroll, S.B. (2002). Reciprocal functions of the *Drosophila* yellow and ebony proteins in the development and evolution of pigment patterns. Development *129*, 1849–1858.

Xiong, G., Tong, X., Gai, T., Li, C., Qiao, L., Monteiro, A., Hu, H., Han, M., Ding, X., Wu, S., et al. (2017). Body shape and coloration of silkworm larvae are influenced by a novel cuticular protein. Genetics *207*, 1053–1066.

Xu, R., Huang, X., Hopkins, T.L., and Kramer, K.J. (1997). Catecholamine and histidyl protein cross-linked structures in sclerotized insect cuticle. Insect Biochem. Mol. Biol. *27*, 101–108.

Zhan, S., Guo, Q., Li, M., Li, M., Li, J., Miao, X., and Huang, Y. (2010). Disruption of an N-acetyltransferase gene in the silkworm reveals a novel role in pigmentation. Development *137*, 4083–4090.

Zhang, L., and Reed, R.D. (2016). Genome editing in butterflies reveals that *spalt* promotes and *Distal-less* represses eyespot colour patterns. Nat. Commun. *7*, 11769.

Zhang, L., Martin, A., Perry, M.W., van der Burg, K.R., Matsuoka, Y., Monteiro, A., and Reed, R.D. (2017a). Genetic basis of melanin pigmentation in butterfly wings. Genetics *205*, 1537–1550.

Zhang, L., Mazo-Vargas, A., and Reed, R.D. (2017b). Single master regulatory gene coordinates the evolution and development of butterfly color and iridescence. Proc. Natl. Acad. Sci. USA *114*, 10707–10712.